Materials Advances

ROYAL SOCIETY OF CHEMISTRY

PAPER

View Article Online
View Journal | View Issue

Cite this: *Mater. Adv.*, 2023, 4, 1989

Preparation of polyaspartamide-based adhesive hydrogels *via* Schiff base reaction with aldehyde-functionalized dextran†

Hend A. Hegazy, ‡[ac] Hwi Hyun Moon,‡[a] Dong-Hyun Lee,[b] Suk Ho Bhang,[b] Youn-Chul Kim,*[b] Changsik Song *[a] and Ji-Heung Kim *[b]

Received 16th January 2023,
Accepted 16th March 2023

DOI: 10.1039/d3ma00032j

rsc.li/materials-advances

Tissue adhesives have become vital candidates for the treatment of injuries, working as hemostatic agents for wound-healing and tissue-sealing. The most accessible commercial adhesives are based on cyanoacrylate and fibrin glue; however, they suffer from drawbacks such as cytotoxicity and poor adhesive strength, which limit their bioapplications. Therefore, the development of an adhesive system that improves tissue repair and closure while exhibiting low cytotoxicity is an important but challenging task. Herein, to overcome the limitations of commercial adhesives, we fabricated biocompatible hydrogels based on amino-functionalized polyaspartamide crosslinked with naturally occurring dextran aldehyde *via* Schiff base chemistry and investigated their adhesive properties. The crosslink density is affected by the ratio between the amine and aldehyde functional groups of each polymer, as well as by the polymer concentrations. We evaluated the adhesive characteristics of the hydrogels using rheometer and lap shear tests. The polyaspartamide-based adhesive hydrogels showed good mechanical strength and self-healing properties and higher adhesive properties than fibrin glue, demonstrating their potential for tissue adhesion applications.

1. Introduction

Tissue adhesives have undergone substantial development with the expansion of the wound care industry.[1,2] However, although several tissue adhesives have reached commercialization in clinical markets, they still have numerous limitations. For instance, despite its excellent tissue adherence, cyanoacrylate adhesive is harmful to cells and poorly biocompatible.[3–5] Meanwhile, fibrin adhesives exhibit biocompatibility but poor mechanical strength and tissue adhesion.[6–8] Ideal tissue adhesives should exhibit not only tissue adhesion properties and good biocompatibility but also mechanically robustness, manoeuvrability, and biodegradability to ensure an efficient removal of staples and sutures during clinical and surgical procedures.[9,10]

Hydrogels are frequently employed as tissue adhesive materials because they physiologically resemble the natural extracellular matrix, which has both static and dynamic crosslinking networks.[11–15] Natural-based hydrogels are promising candidates due to their great biocompatibility; however, their poor stability and mechanical properties limit their applications.[16] Synthetic hydrogels also have an excellent prospect for biomedical applications due to the tunability and reproducibility of their physicochemical or mechanical properties. Unfortunately, they often suffer from poor biocompatibility.[17] In this context, hydrogels consisting of biocompatible polymers, either natural or synthetic, and possessing mechanical and biological activity have emerged as potent platforms for a variety of biomedical applications, including tissue engineering and drug delivery.[18]

As a biocompatible, biodegradable, and low-cytotoxic polymer, polysuccinimide (PSI) has found a wide range of biomedical applications.[19,20] PSI is typically produced by the acid-catalyzed polycondensation of aspartic acid.[21] Because of the labile succinimidyl ring groups in its backbone, PSI undergoes nucleophilic substitution with amine-based molecules, forming polyaspartamide bearing a variety of functional groups with biomedical applications.[22] Due to its protein-like structure, this polymer has a low level of inherent toxicity and degrades into amino acids or small peptides by the action of lysosomal enzymes.[23] Several reports on polyaspartamide-based hydrogels have appeared in recent years, yet they mostly utilized polyaspartamide as the gel-forming macromers with crosslinkable functional groups such as catechol and methacrylate.[24] In other studies, bis-amino

[a] Department of Chemistry, Sungkyunkwan University, Suwon, Gyeonggi 16419, Republic of Korea. E-mail: songcs@skku.edu
[b] Department of Chemical Engineering, Sungkyunkwan University, Suwon, Gyeonggi 16419, Republic of Korea. E-mail: younckim@skku.edu, kimjh@skku.edu
[c] Department of Chemistry, Faculty of Science, Zagazig University, Zagazig, Egypt

† Electronic supplementary information (ESI) available. See DOI: https://doi.org/10.1039/d3ma00032j

‡ These authors contributed equally.

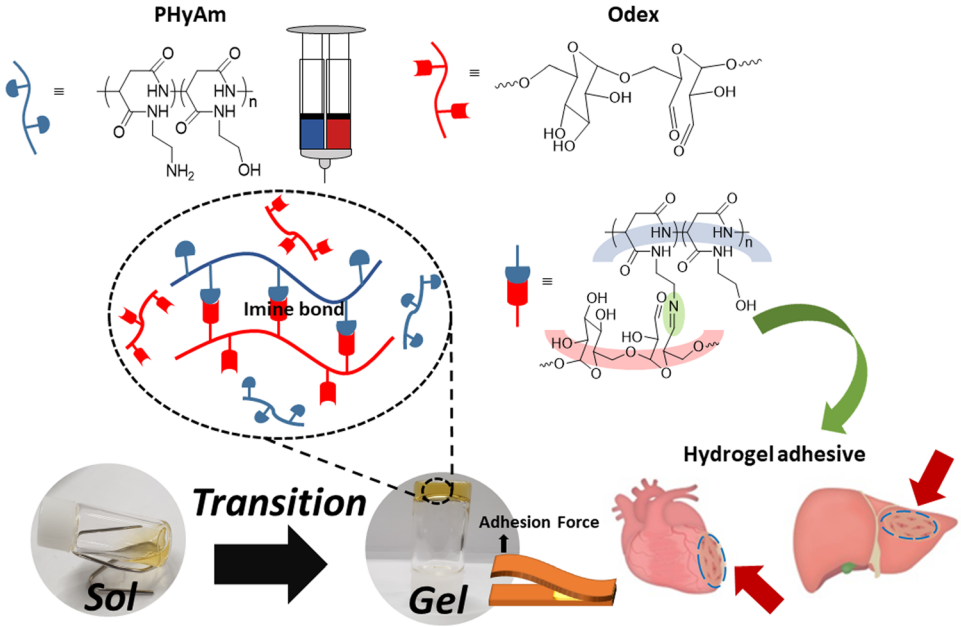

Scheme 1 Schematic diagram of hydrogel formation based on amino-functionalized polyaspartamide (PHyAm) and aldehyde-functionalized dextran (Odex).

compounds were crosslinked with polyaspartamide chains through unopened succinimidyl groups.[25] Additionally, some studies have focused on the synthesis of polyaspartamide-based hydrogels; however, only the mechanical strength and degradability dependence on the degree of substitution have been investigated.[26]

In this study, with the aim of overcoming the drawbacks of commercial adhesives, we fabricated hydrogels using biocompatible polyaspartamide and oxidized dextran (Odex) and investigated their adhesive properties. As shown in Scheme 1, the *in situ* hydrogel was synthesized by coupling an amino-functionalized polyaspartamide (PHyAm) polymer with Odex using a Schiff base reaction. The polyaspartamide polymer was synthesized *via* the ring-opening aminolysis of PSI using ethanolamine (EA) and ethylenediamine (EDA). When aqueous solutions of polyaspartamide and dextran aldehyde polymers were combined at room temperature, gelation occurred at different gelation times depending on the polymer concentration and ratio. Finally, we conducted lap shear and rheometer tests to evaluate the adhesive properties of the synthesized hydrogels. Interestingly, the polyaspartamide-based adhesive hydrogels showed good mechanical strength, self-healing properties, and low cytotoxicity. The adhesive properties of the polyaspartamide-based hydrogels are higher than those of commercial fibrin glue, suggesting its potential use as novel materials in biomedical and wound-healing applications.

2. Materials and methods

2.1. Materials and measurements

Alfa Aesar (MA, USA) supplied L-aspartic acid (98%) and EDA (99%). Phosphoric acid (98%) and EA (99%) were purchased from Acros Organics (MA, USA). Dextran ($M_r \approx 40$ kDa) was provided by Leuconostoc spp. Fibrin glue was purchased from Green Cross (Yongin, Korea). Dialysis tubes with a molecular weight cut off (MWCO) of 3.5–14 000 Da and sodium periodate ($NaIO_4$, 99.8%) were obtained from Sigma–Aldrich (MO, USA Dimethyl sulfoxide (DMSO) was purchased from Samchun chemicals (Seoul, Korea). Distilled water was produced using a Mili-Q water purification system.

^{1}H Nuclear magnetic resonance (NMR) spectra were recorded using a Bruker 500 MHz spectrometer. Fourier transform infrared (FTIR) spectra were recorded on a Vertex70 spectrometer (Bruker Optics, MA, USA) equipped with a diamond attenuated total reflection unit. Scanning electron microscopy (SEM) images were captured on a JEOL 7100 field emission SEM (JEOL, Tokyo, Japan) operated at an accelerating voltage of 15 kV. The rheological properties were investigated using an MCR 302e rheometer (Anton Paar, Graz, Austria). The average molecular weight and polydispersity index of the polymers were determined *via* gel permeation chromatography (GPC) using an Agilent Technology 1260 Infinity equipment (Agilent, CA, USA) with dimethylformamide (DMF) as the eluent and polystyrene as the standard. Lap shear tests were conducted using a universal testing machine (QC-508E, Cometech) with a load cell of 500 N. Cell viability was evaluated using a cell counting kit-8 (CCK-8, Dojindo Molecular Technologies, Inc., Kumamoto, Japan).

2.2. Methods

2.2.1. Synthesis of dextran aldehyde. Oxidized dextran (Odex) was synthesized using the method described by João Maia *et al.*[27] Typically, a solution of 0.264 g of $NaIO_4$ in 2 mL distilled water was added dropwise to a solution of 1.0 g of dextran in 8 mL distilled water to achieve a degree of oxidation of approximately 30%. The reaction was stirred for 6 h at room

temperature and protected from light. To stop the oxidation reaction, an equimolar amount of diethylene glycol was added. The Odex formed was purified *via* dialysis for 3 days against water using a dialysis tube with an MWCO of 3.5–14 000 Da in the dark (water was changed 12 times) and maintained at 4 °C until further need.

2.2.2. Determination of the degree of oxidation. To determine the oxidation degree of Odex, a quantitative reaction between hydroxylamine hydrochloride and the aldehyde groups of Odex was performed as described by Zhao and Heindel.[28] Briefly, 0.1 g of Odex was dissolved in 25 mL (0.25 N) NH_4OH·HCl–methyl orange (0.05%) solution and the mixture was left to dissolve for 2 h at room temperature for the Schiff base reaction to proceed, releasing hydrochloric acid, which was determined by titrating the solution with standard NaOH (0.087 N) until either the pH was 4.0 or the solution became red-yellow (Scheme 2). The oxidation degree was determined as the number of moles of aldehyde generated per mole of dextran monomers in the sample as follows:

$$\%\ \text{Oxidation} = \frac{V_{\text{NaOH}}(\text{mL}) \times 10^{-3} \times M_{\text{NaOH}} \times M_{\text{wt}}(\text{dextran monomer})}{\text{wt}(g)_{\text{Odex}}} \times 100$$

Where V is the volume of NaOH (mL), M the molarity of NaOH (mol L^{-1}), M_{wt} the molecular mass of dextran repeats unit (g mol^{-1}), and wt the weight of Odex (g).

2.2.3. Synthesis of PSI. To synthesize PSI, L-aspartic acid (20 g) and phosphoric acid (20 g) were mixed at room temperature. The mixture was placed in a flask that was attached to a rotary evaporator rotating at a speed of 30–40 rpm, submerged in an oil bath, and equipped with a thermometer. The reaction was conducted by gradually lowering the pressure up to full vacuum while raising the temperature from 25 °C to 200 °C. Once the maximum temperature was reached, the reaction was stirred for almost 5 h. The resulting dark yellow polymer was dissolved in DMF. Then, the polymer solution was precipitated using methanol (1.5 L) and washed with a large amount of methanol. Finally, the solid residue was dried in the oven at 60 °C for 6 h, resulting in a yield of 96%. The weight-average molecular weight of PSI was determined to be 160 000 g mol^{-1} by means of GPC using polystyrene standards and DMF as the eluent.

2.2.4. Synthesis of PHyAm. PHyAm bearing hydroxyl and amine pendant groups was synthesized by conducting the ring-opening aminolysis of PSI using EA and EDA reagents as follows: In a two-necked round-bottom flask, 1 g of PSI was dissolved in 30 mL DMSO under an argon atmosphere. After adding EA (35 and 20 mol% based on the succinimide unit, 0.218 and 0.124 ml, respectively), the mixture was stirred for 24 h at room temperature. Then, excess EDA (1 eq., 0.687 ml) was added, and the reaction was allowed to react for another 12 h. The final solid product was furnished after dialysis purification for three days.

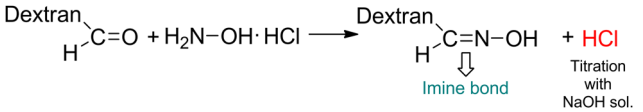

Scheme 2 Determination of the oxidation degree of oxidized dextran (Odex) using the hydroxylamine hydrochloride method.

2.2.5. Preparation of the *in situ* hydrogels. The hydrogels were prepared as follows: 20, 30, and 40 wt% aqueous solutions of PHyAm were mixed with 20, 30, and 40 wt% aqueous solutions of Odex with different mole ratios, *i.e.*, 1 : 0.5, 1 : 1, and 1 : 1.5 ($P_1O_{0.5}$, P_1O_1, and $P_1O_{1.5}$, respectively), and gelation was then achieved at room temperature to obtain the hydrogels. Both the tube inversion method and time sweep analysis of rheometer were used to calculate the gelation times. In the tube inversion method, the gelation time was determined by pouring a hydrogel sample into a vial and inverting it for 5 seconds. Time sweep analysis was performed by mixing PHyAm (20, 30, and 40 wt%) with Odex (20, 30, and 40 wt%) solutions at the rheometer's base plate, where moduli were recorded as a function of time at a 1 rad s^{-1} frequency and 1%. Strain.

2.2.6. Measurement of the swelling ratio of the hydrogels. Freeze-dried hydrogels were weighed to identify the initial mass (W_i). The samples were removed from the solution, surface-dried, and weighed (W_t) at predetermined intervals. The following equation was used to determine the swelling ratio as the equilibrium swelling:

$$\text{Swelling ratio}\ (\%) = \frac{W_t - W_i}{W_i} \times 100$$

2.2.7. Rheometer tests. The rheological properties of the hydrogels were determined *via* dynamic rheology using an Anton Paar rheometer with an 8 mm plate geometry at 25 °C. The hydrogels (8 mm diameter and 1 mm thickness) were prepared. The hydrogel was added onto the lower plate of the rheometer, and the upper plate was lowered to 1 mm gap. To avoid dehydration, oil was then evenly applied over the hydrogel. The measurements were performed in frequency sweep mode by changing the angular frequency from 1 to 100 rad s^{-1} at 1% strain.

2.2.8. Morphology analysis of the hydrogels. Freeze-dried samples coated with platinum were observed by SEM at an accelerating voltage of 15 kV and a current of 20 mA for 60 s to analyze the porous structure of the hydrogels and determine the pore size.

2.2.9. Self-healing properties. Both macroscopic and dynamic rheological techniques were used to assess the self-healing properties of the hydrogels. In the macroscopic method, a mixed solution of PHyAm and Odex polymers was injected into a syringe (8 mm diameter, 3 mm thickness) at room temperature and the fabricated hydrogels were then cut into two pieces using a sharp blade. One of the separate pieces was stained with blue color (disperse blue dye) and brought into contact with the uncolored piece for several minutes at room temperature without any external stimuli. The self-healing ability of the hydrogels was observed and photographed. The self-healing ability of the hydrogel disks (8 mm in diameter, 3 mm in thickness) was further assessed using a

dynamic rheological approach using an alternative strain amplitude sweep model with an angular frequency of 1.0 rad s^{-1}.

2.2.10. Tissue adhesive properties. The adhesive strength of the hydrogels was investigated by performing a lap shear strength experiment using porcine skin (PS) and different substrates.[29,30] In brief, the fats on PS were removed, and the PS sample was cut into a rectangle strip (25 mm wide × 75 mm long) and then immersed in PBS solution for 2 h. After evenly spreading 60 μL of PHyAm and Odex solutions over an area of 12.5 × 25 mm of one strip and covering it with a second strip, the sample was allowed to sit for 30 min to reach full gelation. The hydrogel was allowed to adhere to the PS using a 2000 g weight. Lap shear tests with a 500 N load cell were conducted to determine the adhesive strength with a 60 mm min^{-1} displacement rate. Tests were performed in triplicate and averaged. Moreover, the adhesion strength on different substrates such as glass, polymethylmethacrylate (PMMA) and polyethylene terephthalate (PET) plastics, and aluminum foil (25 mm wide × 75 mm long) was measured using the same method.

2.2.11. Cytotoxicity of the hydrogels. The CCK-8 assay measures the amount of formazan dye that is reduced by the action of intracellular dehydrogenase. The number of living cells is proportional to the amount of formazan dye. Here, hDFs (2×10^4 cells per well with 400 μL serum free medium) in passage 7 were cultured on 24-well transwell plates (SPL Insert Hanging, SPL Life Sciences, Pocheon, South Korea) with various amounts of the hydrogel for 24 h and then rinsed with PBS thrice. After replenishing the wells with fresh medium, CCK-8 solution was added to each well, and the cells were incubated for 2 h. Finally, the absorbance was measured at 450 nm using a plate reader (Infinite F50, Tecan, Männedorf, Switzerland). The cell viability was calculated as the percentage of viable cells relative to hydrogel-untreated cells (n = 4 per group).

3. Results and discussion

3.1. Synthesis and characterization of the PHyAm/Odex hydrogels

For a variety of injuries, tissue adhesives have emerged as a promising contender, acting as hemostatic, tissue-sealing, and wound-healing agents. Thus, developing an adhesive system that can enhance tissue repair and closure with low cytotoxicity is highly desirable.[31] Here, a hydrogel composed of PHyAm and Odex polymers was used to synthesize an injectable and self-healing hydrogel dressing with excellent adhesive properties.

First, as shown in Scheme 3a, PSI was synthesized using the amino acid L-aspartic acid. Then, the PHyAm polymer was synthesized *via* an aminolysis reaction of PSI using EA and EDA (Scheme 3b). Subsequent experiments were conducted with an EA : EDA ratio of 3 : 7 because polymers having a higher EDA content may react with Odex. The structures and compositions

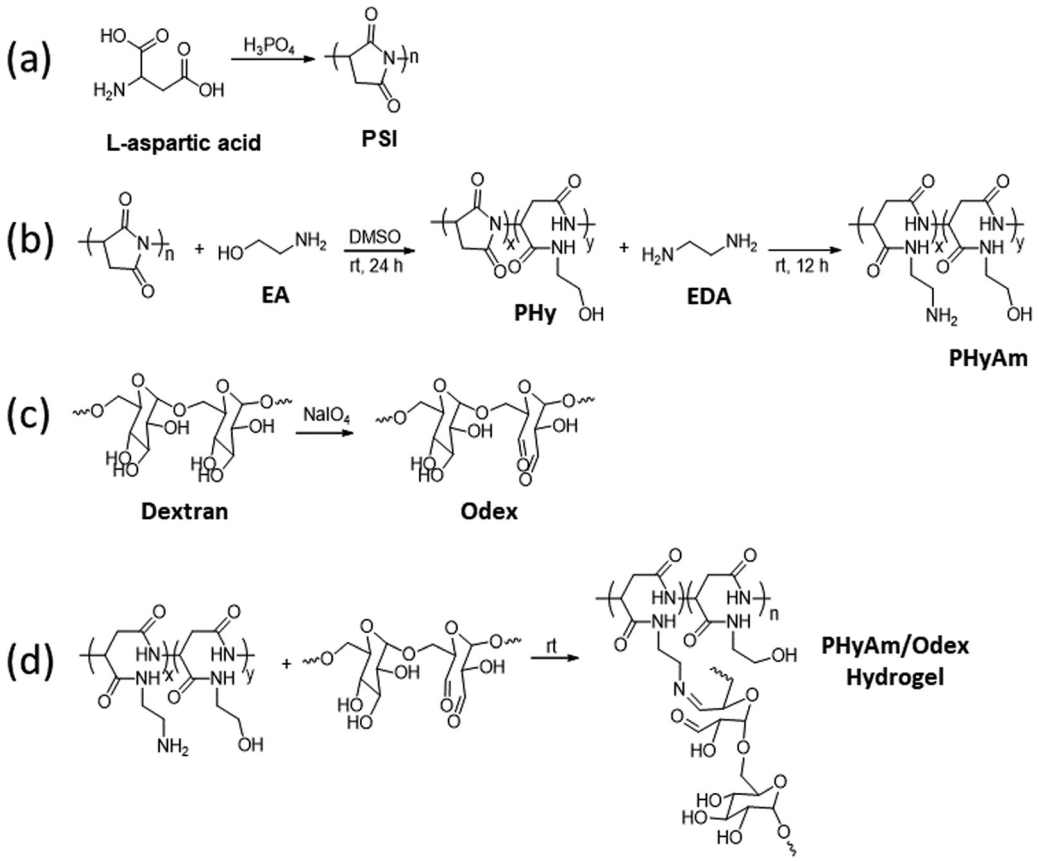

Scheme 3 Synthetic route to (a) PSI, (b) PHyAm, (c) Odex, and (d) the PHyAm/Odex hydrogel.

of PSI and the PHyAm polymers were confirmed by ^{1}H NMR spectroscopy using D_2O as the solvent (Fig. S1, ESI†).

Second, Odex was synthesized by oxidizing vicinal diols using $NaIO_4$ as the oxidizing agent (Scheme 3c). As depicted in Fig. S2 (ESI†), the ^{1}H NMR spectrum of Odex showed multiple new peaks at 5.0–6.0 ppm belonging to the hemiacetal structures of the aldehyde groups, which are absent in the ^{1}H NMR spectrum of dextran, demonstrating the successful synthesis of Odex. Moreover, the FTIR spectrum showed a significant peak at 1748 cm^{-1} characteristic of a carbonyl group, confirming the chemical structure (Fig. S3, ESI†). Importantly, the oxidization degree of dextran aldehyde was found to be 30% using the hydroxylamine hydrochloride method.

The PHyAm/Odex hydrogels were easily synthesized by mixing an aqueous solution of PHyAm with an Odex solution at room temperature (Scheme 3d). Interestingly, a pale-yellow gel was formed within a few seconds without any external stimulus. This *in situ* gelation of the PHyAm/Odex mixture occurred *via* a Schiff base reaction, which resulted in the formation of imine bonds, as confirmed by FTIR analysis which showed a distinct peak at 1647 cm^{-1} corresponding to imine bond (Fig. S3, ESI†).

3.2. Analysis of the physical properties of the hydrogels

The gelation time of hydrogels is crucial to their practical biomedical application. Since surgery requires a definite time, a short gelation time is undesirable, whereas a long gelation time hinders closing promptly the wound site.[32] In this study, the gelation time was determined by the tube inversion method[33,34] and rheological measurements.[33] It was observed in both methods that the gelation time increased with decreasing crosslinker concentration. As shown in (Fig. 1a), the gelation time decreased from near 180 s to 20 s by increasing the crosslinker concentration from 20 to 40 wt% for $P_1O_{1.5}$ hydrogel because of the gradually enhanced crosslinking density of the hydrogels. The extremely quick setting of the 40% hydrogel could be advantageous for preventing the gel from spreading to nearby tissues. Similar results were observed in rheological measurements using oscillation time sweep test, in which the gelation point was determined as the time at which G' and G'' crossed each other (Fig. S4, ESI†). The mechanical strength of hydrogels is also important to shield the wound from further injuries.[35] To assess the rheological characteristics of the hydrogels, the frequency dependence of the storage (G') and loss (G'') modulus was observed at angular frequencies between 1 and 100 rad s^{-1} and 1% strain. In all samples, G' was much greater than G'' throughout the frequency range, which suggested that the hydrogels were highly stable and elastic. Additionally, the precursor concentrations and ratios were found to influence the final stiffness of the hydrogels. Thus, the 40 wt% hydrogel (33 kPa) exhibited higher final moduli and faster gelation time than the 30 wt% hydrogel (23 kPa) and the 20 wt% hydrogel (7 kPa) due to the increase in the crosslinking densities with increasing the PHyAm and Odex concentration, hence increasing the stiffness of the hydrogel (Fig. 1b and Fig. S5a–c, ESI†). The damping factor of the hydrogels was found to be less than 1, demonstrating their elastic nature (Fig. S5d, ESI†).

Furthermore, as revealed by an SEM analysis, all the hydrogels showed interconnected porous structures (Fig. 1d and Fig. S6a, b, ESI†). The corresponding mean pore diameter significantly decreased from 1.721 to 1.183 μm with increasing the concentration of the hydrogels from 20 to 40 wt% for $P_1O_{1.5}$.

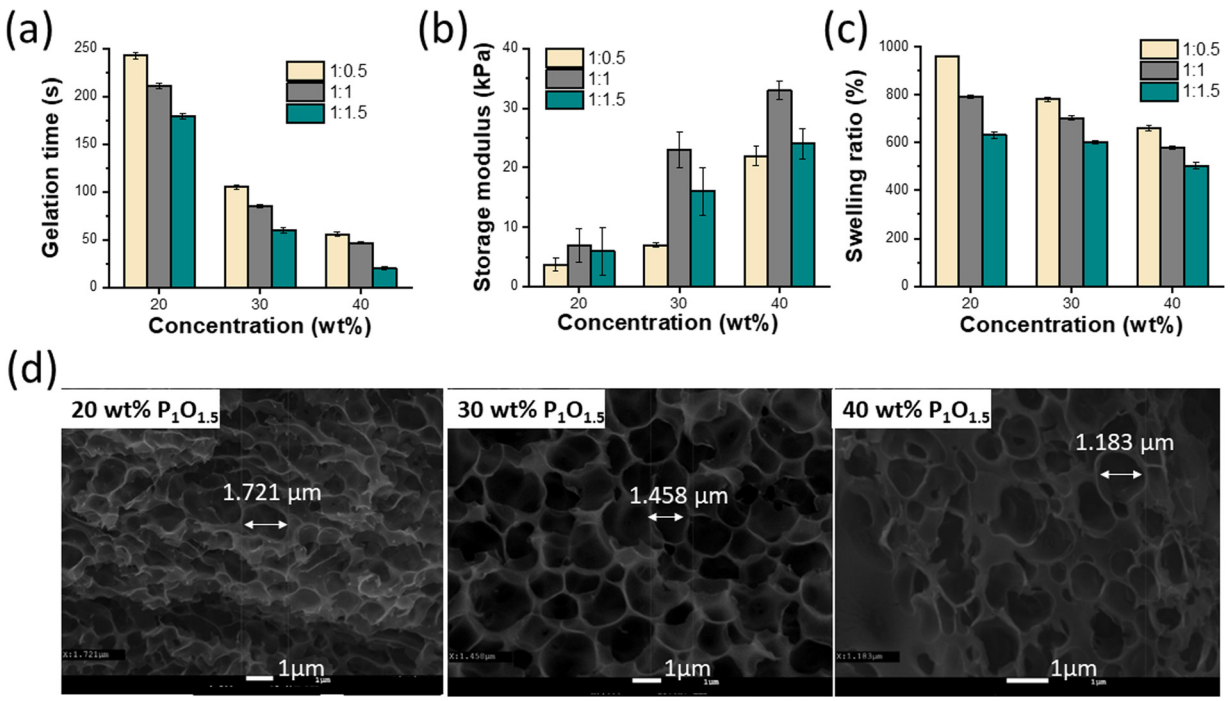

Fig. 1 (a) Gelation time, (b) frequency dependence of the storage (G') and loss (G'') modulus, (c) swelling ratio of the hydrogels formed at concentrations of 20, 30, and 40 wt%. (d) SEM images of the $P_1O_{1.5}$ hydrogels formed at concentrations of 20, 30, and 40 wt%.

It is well known that the pore volume and pore size of porous materials can be mostly controlled by the crosslink density in the hydrogel network.

3.3. Swelling studies

Swelling is a frequent characteristic of hydrophilic polymer adhesives and vital for hydrogels with prospective applications in biomedical fields because they are exposed to biological fluids and can be harmful to adhesion and to adjacent tissues.[36] When water is absorbed into the adhesive matrix, the density of the polymer decreases, which might result in the volumetric expansion of adhesives during swelling, which in turn compresses the nearby tissue mechanically. Basically, many factors affect the swelling process, such as the nature of the polymer, the rigidity of the polymer chain, its ability to expand, and the degree of crosslinking. The swelling properties of the proposed hydrogels at different ratios and concentrations are shown in Fig. 1c. These results demonstrated that the equilibrium swelling ratios decreased with increasing concentration (20–40 wt%) and ratio (1 : 05–1 : 1.5), indicating increase in the crosslinking density accordingly.

3.4. Self-healing properties of the hydrogels

Hydrogel wound dressings can withstand external mechanical strain after being applied to the wound site. Therefore, using self-healing hydrogels as wound dressings can extend their durability.[37] To evaluate the self-healing ability of the hydrogels, a hydrogel sample formed into a cylindrical shape with a diameter of 8 mm and a thickness of roughly 3 mm was cut into two pieces, which were then brought into contact and allowed to self-heal. After 5–10 min, the rebuilt hydrogel disk was lifted using tweezers to confirm its ability to keep integrity under gravity (Fig. 2a), which can be attributed to the reversible dynamic covalent bonds (imine bonds) within the hydrogel network migrating to the interfacial chains to undergo recrosslinking. The self-healing properties of the hydrogels were further confirmed by means of a dynamic rheological analysis. The critical strain point near which the hydrogel changes from solid to liquid state was determined using a strain amplitude sweep test. As shown in Fig. 2b, at low strain, G' and G'' had constant values. Then, upon increasing the strain, the G' and G'' curves intersected at about 3.8% strain, which is the critical point. Further increasing the strain up to 10% led to a sharp decrease in the G' value below the G'' value, demonstrating the collapse of the hydrogel network. After 5 min, the strain amplitude sweep test was repeated on the same sample to check the self-healing ability, which was about 60% of the value obtained in the first measurement. These findings showed that the PHyAm/Odex hydrogels have considerable self-healing abilities due to the formation of imine bonds between the amine groups of PHyAm and the aldehyde groups of Odex.

3.5. Adhesive properties of the hydrogels

The adhesion properties of hydrogel dressings are critical in the wound-healing process because it controls bleeding and prevents gas or fluid leakage from injured sites.[38–40] Tissue adhesive polymers containing aldehyde groups have been utilized extensively. In the case of Odex, the aldehyde groups can react with the amino groups in tissues to create chemical linkages for adhesion.[38] To quantify the adhesion behaviour of the PHyAm/Odex hydrogels, a widely used lap shear test method was employed. Among the many parameters that affect adhesion, the substrate to which the material is adhered is one of the critical factors.[41] Fig. 3a shows the preparation of the sample for lap shear testing on different substrates. In general, substrates can be divided into low-surface-energy plastics and high-surface-energy metals. Typically, a strong adhesion is more favoured on high-energy, rough surfaces.[41] Fig. 3b shows the immediate bulk adhesive strengths for various substrates commonly used as daily-life materials (aluminum foil, glass, and plastic). The highest adhesive strength values of 131, 74, 65, and 58 kPa for glass, PMMA, aluminum, and PET plastic substrate, respectively, were obtained at a 40 wt% P_1O_1 hydrogel. The best adherence was observed on glass substrates, which might be due to the formation of strong hydrogen bonds between the amine groups of the hydrogel and the hydroxyl groups of glass (Si–OH).[42] For PET and PMMA plastics, attractive interactions caused by dipole–dipole interactions and hydrogen bonds between polyaspartamide and the ester groups (hydrogen acceptors) of PET and PMMA may be responsible for the observed adhesive properties.[43]

The adhesion strength of the hydrogels as a function of the aging time on a glass slide is depicted in Fig. S7a (ESI†). As the aging time increased from 10 min to 24 h, the adhesive strength

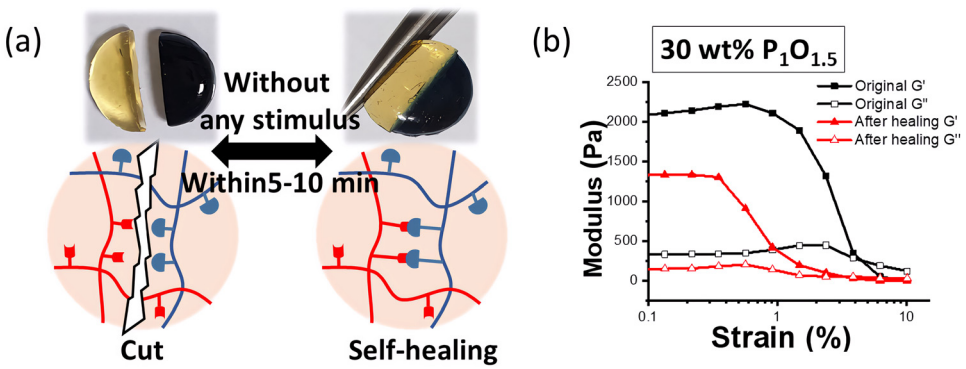

Fig. 2 (a) Diagram of macroscopic analysis of the self-healing property of the hydrogels. (b) rheological analysis of self-healing recovery after 5 min.

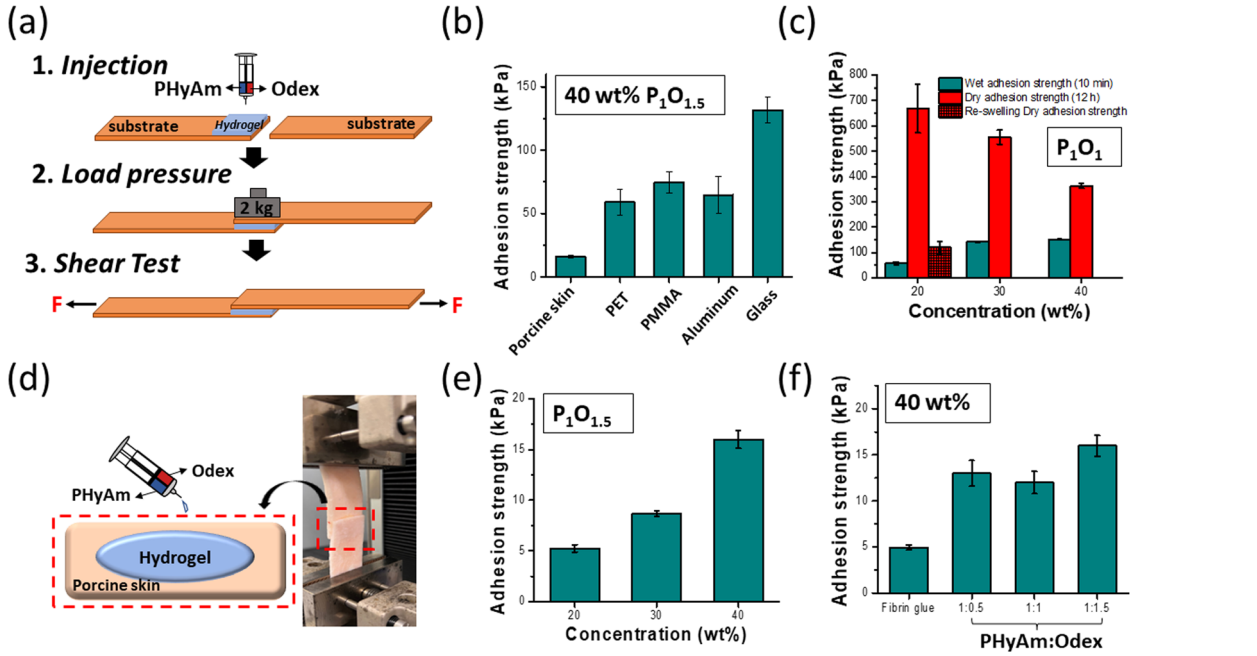

Fig. 3 (a) Schematic illustration of adhesion strength measurements. (b) Adhesion strength of a 40 wt% $P_1O_{1.5}$ hydrogel measured using various substrates under wet condition. (c) Adhesion strength of 20, 30, and 40 wt% P_1O_1 hydrogels on glass substrates under wet and dry conditions. (d) Image of the lap shear test using porcine skin. (e) Wet adhesion strength of 20, 30, and 40 wt% $P_1O_{1.5}$ hydrogels on porcine skin. (f) Wet adhesion strength of hydrogels with various hydrogels ($P_1O_{0.5}$, P_1O_1, $P_1O_{1.5}$) and fibrin glue.

increased up to 1.26 MPa after 24 h. Fig. 3c shows the adhesive strength of PHyAm/Odex hydrogels with different polymer concentrations on a glass substrate after 10 min and 12 h. After 10 min, the adhesive strength increased from 57 kPa to 150 kPa upon increasing the concentration from 20 to 40 wt%. Whereas it decreased from 668 kPa to 363 kPa by increasing the concentration from 20 to 40 wt% after 12 h, which probably due to the dehydration of the hydrogel with time. Moreover, the adhesion properties of different ratios of the hydrogel after 10 min and after 12 h (Fig. S7b and c, ESI†), respectively showed that P_1O_1 has the highest adhesion properties. The results of the lap shear adhesion tests and the G' value of the hydrogel derived from rheological measurements, which evaluate the cohesion strength of materials, were in good agreement.

The adhesion ability of the hydrogels was then compared with clinically administered fibrin glue as a positive control using PS, which is commonly used for adhesive testing in biomedical applications owing to its similarity to the human dermis.[44] Fig. 3d depicts a schematic illustration and a typical image for the lap shear strength test. After spreading the hydrogels on the PS surface, the samples were overlaid and compressed by a weight of 2000 g for 30 min. With increasing the PHyAm/Odex concentration from 20 to 40 wt%, the adhesive strength increased from about 5 to 16 kPa (Fig. 3e). The adhesion to PS might result from the formation of hydrogen bonds between the polymer and the hydroxyl, amine, and carboxyl functional groups present on PS.[45] As shown in Fig. 3f, the tissue adhesion was measured using different PHyAm:Odex mole ratios ($P_1O_{0.5}$, P_1O_1, and $P_1O_{1.5}$), finding that the hydrogel with a $P_1O_{1.5}$ exhibited much higher adhesive properties. This could be attributed to the following factors: (1) the higher Odex ratio provides more aldehyde groups for the reaction with the amino groups of the PS tissue, resulting in bonding;[46] (2) the robust cohesion of the hydrogel network improves the adhesion strength on PS. Additionally, in order to evaluate the feasibility and applicability of our adhesive polymers, wet and dry adhesion strength properties have been investigated using porcine skin tissue and the results showed that there are no noticeable differences in both cases (Fig. S7d, ESI†), indicating the real applicability of the prepared polymers in real biofields. In these

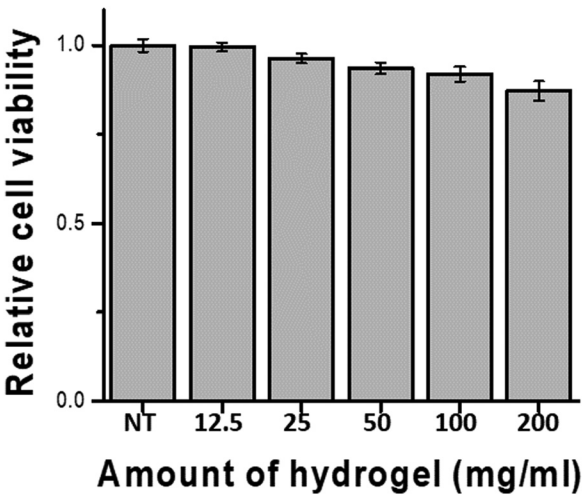

Fig. 4 Cell viability test of the 30 wt% $P_1O_{1.5}$ hydrogel (NT: no treatment).

measurements, all the hydrogels showed stronger adherence than the commercial adhesive fibrin glue (4.95 kPa).

3.6. Cytotoxicity of the hydrogels

Biocompatibility studies were conducted in 24-well transwell plates using different amounts (5, 10, 20, 40, and 80 mg) of hydrogel in the transwell and 400 μL of medium in the peripheral well. The results depicted in Fig. 4 were obtained by measuring the cell viability after 24 h of incubation. Even high amounts of hydrogel showed 85% or more viability compared with the blank experiment (no treatment). Reducing cell viability by more than 30% is defined as a cytotoxic effect by International Standard ISO 10993-5 (2009),[47] demonstrating that the hydrogel did not exert a severe cytotoxic effect on hDF cell.

Conclusion

In this work, adhesive hydrogels were synthesized by forming imine bonds *via* a Schiff base reaction between the amine functional groups of polyaspartamide and the aldehyde groups of dextran. The rheological and adhesive properties of hydrogels synthesized at various concentrations and ratios of amines and aldehydes were analyzed, finding that the 20 wt% hydrogel had high wet adhesion and the 40% hydrogel exhibited high dry adhesion. Among the various surfaces evaluated, glass showed the highest adhesion when the $P_1O_{0.5}$ hydrogel, while PS showed the highest adhesion when the $P_1O_{1.5}$ hydrogel. The synthesized hydrogels exhibited self-healing properties within 5–10 min without any external stimuli, as well as low cytotoxicity. Notably, the synthesized hydrogels exhibited higher adhesive strength on PS than fibrin glue, which is currently used as a skin adhesive. Therefore, this work demonstrates the potential of polyaspartamide-based adhesive hydrogels as biomedical adhesives in clinical applications.

Author contributions

H. A. Hegazy: conceptualization, investigation, formal analysis, writing – original draft; H. H. Moon: conceptualization, investigation, data curation, writing – original draft; D. H. Lee: data curation; S. H. Bhang: supervision; Y. C. Kim: conceptualization, investigation, writing – review & editing, supervision; C. S. Song: conceptualization, investigation, writing – review & editing, supervision; J. H. Kim: conceptualization, investigation, supervision.

Conflicts of interest

There are no conflicts to declare.

Acknowledgements

This work was supported by the Materials and Components Technology Development Program (Project No. 20013223) and the Technology Innovation Program (Project No. 20013794, Center for Composite Materials and Concurrent Design) funded by the Ministry of Trade, Industry & Energy (MOTIE, KOREA).

References

1 S. Nam and D. Mooney, *Chem. Rev.*, 2021, **121**, 11336–11384.
2 M. B. Detweiler, J. G. Detweiler and J. Fenton, *J. Invest. Surg.*, 1999, **12**, 245–262.
3 G. Pascual, S. Sotomayor, M. Rodriguez, B. Perez-Kohler, A. Kuhnhardt, M. Fernandez-Gutierrez, J. San Roman and J. M. Bellon, *PLoS One*, 2016, **11**, e0157920.
4 B. Mizrahi, C. F. Stefanescu, C. Yang, M. W. Lawlor, D. Ko, R. Langer and D. S. Kohane, *Acta Biomater.*, 2011, **7**, 3150–3157.
5 B. J. Vote and M. J. Elder, *Clin. Exp. Ophthalmol.*, 2000, **28**, 437–442.
6 G. Lopezcarasa-Hernandez, J.-F. Perez-Vazquez, J.-L. Guerrero-Naranjo and M. A. Martinez-Castellanos, *Int. J. Retina Vitreous*, 2021, **7**, 33.
7 M. Radosevich, H. I. Goubran and T. Burnouf, *Vox Sang.*, 1997, **72**, 133–143.
8 K. Conrad and A. Yoskovitch, *Arch. Facial Plast. Surg.*, 2003, **5**, 522–527.
9 X. Zhang, Y. Jiang, L. Han and X. Lu, *Biosurface and Biotribology*, 2021, **7**, 163–179.
10 R. Yu, M. Li, Z. Li, G. Pan, Y. Liang and B. Guo, *Adv. Healthcare Mater.*, 2022, **11**, 2102749.
11 Y. Yi, C. Xie, J. Liu, Y. Zheng, J. Wang and X. Lu, *J. Mater. Chem. B*, 2021, **9**, 8739–8767.
12 H. Geckil, F. Xu, X. Zhang, S. Moon and U. Demirci, *Nanomedicine*, 2010, **5**, 469–484.
13 M. Okawa, A. Tanabe, S. Ohta, S. Nagatoishi, K. Tsumoto and T. Ito, *Commun. Mater.*, 2022, **3**, 81.
14 A. Sigen, Q. Xu, M. Johnson, J. Creagh-Flynn, M. Venet, D. Zhou, I. Lara-Sáez, H. Tai and W. Wang, *Appl. Mater. Today*, 2021, **22**, 100967.
15 Y. Liang, M. Li, Y. Yang, L. Qiao, H. Xu and B. Guo, *ACS Nano*, 2022, **16**, 3194–3207.
16 M. Klein and E. Poverenov, *J. Sci. Food Agric.*, 2020, **100**, 2337–2347.
17 U. S. K. Madduma-Bandarage and S. V. Madihally, *J. Appl. Polym. Sci.*, 2021, **138**, 50376.
18 J. Jang and C. Cha, *Biomacromolecules*, 2018, **19**, 691–700.
19 H. Adelnia, I. Blakey, P. J. Little and H. T. Ta, *Front. chem.*, 2019, **7**, 755.
20 H. Adelnia, H. D. N. Tran, P. J. Little, I. Blakey and H. T. Ta, *ACS Biomater. Sci. Eng.*, 2021, **7**, 2083–2105.
21 T. Nakato, A. Kusuno and T. Kakuchi, *J. Polym. Sci., Part A: Polym. Chem.*, 2000, **38**, 117–122.
22 E. Jalalvandi and A. Shavandi, *Eur. Polym. J.*, 2018, **109**, 43–54.
23 G. Pitarresi, F. S. Palumbo, G. Giammona, M. A. Casadei and F. Micheletti Moracci, *Biomaterials*, 2003, **24**, 4301–4313.
24 G. Pitarresi, P. Pierro, G. Tripodo, D. Mandracchia and G. Giammona, *J. Drug Delivery Sci. Technol.*, 2005, **15**, 377–382.

25 J. R. Moon and J.-H. Kim, *Macromol. Res.*, 2008, **16**, 489–491.
26 M. Kim and C. Cha, *Biomacromolecules*, 2020, **21**, 3693–3703.
27 J. Maia, R. A. Carvalho, J. F. J. Coelho, P. N. Simões and M. H. Gil, *Polymer*, 2011, **52**, 258–265.
28 H. Zhao and N. D. Heindel, *Pharm. Res.*, 1991, **8**, 400–402.
29 D. Lu, H. Wang, T. Li, Y. Li, F. Dou, S. Sun, H. Guo, S. Liao, Z. Yang, Q. Wei and Z. Lei, *ACS Appl. Mater. Interfaces*, 2017, **9**, 16756–16766.
30 Y.-z Bu, G.-f Sun, L.-c Zhang, J.-h Liu, F. Yang, P.-f Tang and D.-c Wu, *Chin. J. Polym. Sci.*, 2017, **35**, 1231–1242.
31 A. Bal-Ozturk, B. Cecen, M. Avci-Adali, S. N. Topkaya, E. Alarcin, G. Yasayan, Y.-C. Ethan, B. Bulkurcuoglu, A. Akpek, H. Avci, K. Shi, S. R. Shin and S. Hassan, *Nano Today*, 2021, **36**, 101049.
32 X. Yang, G. Liu, L. Peng, J. Guo, L. Tao, J. Yuan, C. Chang, Y. Wei and L. Zhang, *Adv. Funct. Mater.*, 2017, **27**, 1703174.
33 C. T. Huynh, Z. Zheng, M. K. Nguyen, A. McMillan, G. Yesilbag Tonga, V. M. Rotello and E. Alsberg, *ACS Biomater. Sci. Eng.*, 2017, **3**, 2011–2023.
34 M. K. Nguyen, O. Jeon, M. D. Krebs, D. Schapira and E. Alsberg, *Biomaterials*, 2014, **35**, 6278–6286.
35 X. Du, Y. Liu, X. Wang, H. Yan, L. Wang, L. Qu, D. Kong, M. Qiao and L. Wang, *Mater. Sci. Eng., C*, 2019, **104**, 109930.
36 Q. Chai, Y. Jiao and X. Yu, *Gels*, 2017, **3**, 6.
37 X. Zhao, H. Wu, B. Guo, R. Dong, Y. Qiu and P. X. Ma, *Biomaterials*, 2017, **122**, 34–47.
38 C. Ghobril and M. W. Grinstaff, *Chem. Soc. Rev.*, 2015, **44**, 1820–1835.
39 N. Annabi, K. Yue, A. Tamayol and A. Khademhosseini, *Eur. J. Pharm. Biopharm.*, 2015, **95**, 27–39.
40 E. Y. Jeon, B. H. Hwang, Y. J. Yang, B. J. Kim, B. H. Choi, G. Y. Jung and H. J. Cha, *Biomaterials*, 2015, **67**, 11–19.
41 M. Guvendiren, D. A. Brass, P. B. Messersmith and K. R. Shull, *J. Adhes.*, 2009, **85**, 631–645.
42 G. Bovone, O. Y. Dudaryeva, B. Marco-Dufort and M. W. Tibbitt, *ACS Biomater. Sci. Eng.*, 2021, **7**, 4048–4076.
43 M. A. Sibeko, M. L. Saladino, A. S. Luyt and E. Caponetti, *J. Mater. Sci.*, 2016, **51**, 3957–3970.
44 H. Chung and R. H. Grubbs, *Macromolecules*, 2012, **45**, 9666–9673.
45 X. Pei, J. Wang, Y. Cong and J. Fu, *J. Polym. Sci.*, 2021, **59**, 1312–1337.
46 J. Hoque, R. G. Prakash, K. Paramanandham, B. R. Shome and J. Haldar, *Mol. Pharmaceutics*, 2017, **14**, 1218–1230.
47 D. Zhou, S. Li, M. Pei, H. Yang, S. Gu, Y. Tao, D. Ye, Y. Zhou, W. Xu and P. Xiao, *ACS Appl. Mater. Interfaces*, 2020, **12**, 18225–18234.